Histol Histopathol (2010) 25: 1025-1038

**http://www.hh.um.es**

**Histology and Histopathology**

*Cellular and Molecular Biology*

# Immunohistochemical study of macrophage and cytokine dynamics in the gut of scrapie-infected mice

**José Lorenzo Romero-Trevejo[1], José Carlos Gómez-Villamandos, Miriam Pedrera, Alfonso Blanco, María José Bautista and Pedro José Sánchez-Cordón**

Department of Comparative Pathology, Faculty of Veterinary Medicine, University of Córdoba, Córdoba, Spain

[1]Present address: Division of Hepatology and Gene Therapy, Center for Applied Medical Research (CIMA), University of Navarra, Pamplona, Spain

**Summary.** To study numerical changes in intestinal macrophages and variations in cytokine production by immune cells in the intestine, conventional C57BL/6J mice were orally infected with the Rocky Mountain Laboratory strain of scrapie. Animals were sacrificed at different timepoints, and samples were taken and processed by routine methods for morphological and immunohistochemical analysis. The results point to a possible role for macrophages in the uptake and transport of the infective agent to Peyer's patches. The observed increase in macrophage numbers in subepithelial sites, taken in conjunction with a drop in tumour necrosis factor-α production at these sites, suggests a possible secretory inhibition that could be induced by the disease-associated prion protein (PrPd). On the other hand, cytokine dynamics indicated the presence of an impaired Th1-Th2 cell mediated response, which could facilitate the spread of PrPd to the central nervous system. Further research is required to confirm these hypotheses.

**Key words:** Scrapie, Cytokines, Immune response, Gut-associated lymphoid tissues, Pathology

## Introduction

Transmissible spongiform encephalopathies (TSEs) constitute a group of fatal neurodegenerative diseases caused by the accumulation of a conformationally-changed prion protein. This change results from a conversion of part of the α-helix structure into ß-sheet secondary structures (Prusiner, 1998). Animal TSEs include scrapie in sheep and goats, and bovine spongiform encephalopathy or chronic wasting disease, whereas Creutzfeldt-Jakob disease and its variant, Gerstmann-Sträussler-Scheinker syndrome, familial fatal insomnia and kuru affect human beings. The accumulation of this ß-sheet-rich isoform or PrPd in the central nervous system (CNS) is responsible for the most common pathologies in these diseases, including glial activation, neuronal loss, amyloidal aggregation, and spongiform changes in neurons and neuropil (Chesebro, 2003), which give rise to the neural clinical signs typical of TSEs.

It is commonly accepted that, after a natural or experimental oral infection, PrPd accumulates in cells of the lymphoreticular system, such as tingible body macrophages and follicular dendritic cells, in gut-associated lymphoid tissue (GALT) and in mesenteric lymphnodes, before spreading to the CNS through peripheral nerves in the intestinal wall (Beekes and McBride, 2000; Van Keulen et al., 2000; Jeffrey et al., 2006). From the CNS, PrPd can subsequently reach other tissues, e.g. muscles, by centrifugal diffusion (Beekes and McBride, 2007). Despite the importance of understanding the pathogenesis of TSEs, and despite their public-health significance, few *in vivo* studies have focused on the mechanisms of these diseases at natural entry sites (González et al., 2005; Glaysher and Mabbott, 2007; Raymond et al., 2007; Krüger et al., 2009).

For years, the absence of an overt inflammatory response was a commonly-accepted feature of prion diseases. Currently, however, inflammation of neural tissues, albeit an atypical response, is regarded as a cardinal sign of TSEs (Perry et al., 2002; Thackray et al., 2004), and a role for cytokines and inflammatory mediators in the neural pathogenesis of prion diseases has been proposed by a number of authors (Campbell et

*Offprint requests to:* José Lorenzo Romero-Trevejo, Departamento de Anatomía y Anatomía Patológica Comparadas, Edificio Sanidad Animal, Campus de Rabanales, 14014 Córdoba, España. e-mail: v82rotrj@uco.es

al., 1994; Williams et al., 1994, 1997; Giese et al., 1998; Peyrin et al., 1999; Veerhuis et al., 2002; Thackray et al., 2004). However, despite the findings reported for neural tissues, comparatively little attention has been paid to the role of chemical mediators produced by intestinal macrophages, a major immunocompetent-cell population involved in mucosal immunity against foreign antigens. In addition to their role in the clearance of cell debris, intestinal macrophages play an important part in the initiation of inflammation. Moreover, intestinal macrophages and follicular dendritic cells are also responsible for antigen-presenting processes and for the onset of the local immune response through the liberation of various chemical mediators (Platt and Mowat, 2008; Rescigno et al., 2008). Strikingly little appears to be known about the role of these chemical mediators at the entry sites for TSEs, in spite of the importance of the intestine and GALT as defence mechanisms against oral pathogens.

The purpose of this study was to evaluate the spatial and temporal relationship between the presence and distribution of PrPd in GALT and the quantitative changes and biosynthetic activation of intestinal macrophages and other immune cells in this location in an experimental murine model, in order to ascertain the local immune response and to throw light on the pathogenesis of prion diseases.

## Materials and methods

### *Animals*

A hundred and fifty conventional healthy female C57BL/6J mice, aged 4 to 6 weeks, and weighing approximately 18 g, were used in this study. Animals were housed according to the European Community guidelines on animal scientific research.

### *PrPd and control inocula*

Twelve Rocky Mountain Laboratory (RML) mouse brains, previously confirmed positive, were supplied by the Centro de Investigación en Sanidad Animal (CISA-INIA, Valdeolmos, Madrid, Spain). Brains were pooled and diluted 1:10 in a commercial lipoid emulsion to be used as infective inoculum. Twelve normal mouse brains were pooled and diluted as above to inoculate mock mice.

### *Inoculation and monitoring*

In order to better reproduce the natural route of infection of TSEs, one hundred and two 24-hour-fasted mice were individually placed and orally fed with 300 $\mu$l of infective brain homogenate through an Eppendorf tube. After fully consuming the homogenate, mice were housed in batches of 6 until sacrifice. As negative controls, 4 groups of 6 mice were fed as described with 300 $\mu$l of normal brain homogenate (control group 1) and 4 other groups of 6 mice were not inoculated (control group 2). To evaluate clinical signs appearing after inoculation, mice were observed weekly and their neurological status, loss of appetite and postural disorders were assessed.

### *Sacrifice, necropsy and specimen processing*

PrPd-inoculated animals were sacrificed by cervical dislocation in batches of 6 at 15, 35, 45, 60, 75, 90, 105, 120, 150, 180, 210, 240 and 270 days post-inoculation (dpi). Mice originally designed to be killed at 300, 350 and 400 dpi were all sacrificed between 270 and 300 days for ethical reasons. Normal brain-inoculated animals (NBI) and non-inoculated animals (NI) were also sacrificed in batches of 6 at 0, 35, 90 and 270 dpi, in order to cover the whole experimental period. Samples from the distal small intestine – including Peyer's patches (PPs) –, mesenteric lymphnodes and brain were taken and fixed for 24 hours in 10% buffered formalin solution (pH 7.2) and zinc salt fixative. Subsequently, samples were dehydrated through a graded series of alcohol to xylol and routinely embedded in paraffin-wax for histopathological and immunohistochemical examination.

Additionally, samples from the distal small intestine were taken and fixed in 2.5% glutaraldehyde (0.1 M) in phosphate buffer saline (pH 7.2), postfixed in 2% osmium tetroxide, dehydrated in acetone and embedded in epoxyresins for ultrastructural analysis.

### *Histopathological, ultrastructural and immunohistochemical analyses*

For histopathological analysis, 5-$\mu$m wax-embedded sections of 10% buffered formalin solution-fixed tissues from the distal small intestine were cut and stained with hematoxylin and eosin. Samples were then evaluated through a light microscope.

For ultrastructural examination, 50-nm sections of 2.5% glutaraldehyde-fixed tissues from the distal small intestine were counterstained with uranyl acetate and lead citrate, and viewed through a transmission electron microscope.

For immunohistochemical analysis, the avidin-biotin-peroxidase complex method was used to immunolabel the different antigens. To characterize the evolution and dynamics of the disease among the different target organs, PrPd was demonstrated on 3-$\mu$m sections of 10% buffered formalin-fixed samples from the distal small intestine, mesenteric lymphnodes and brain using the polyclonal antibody Rb482. This antibody reacts with the 221-233 residues of the bovine PrP. Heat epitope-retrieval treatment was performed by citrated autoclaving (pH 6.1). Brain sections from previously scrapie positive-confirmed mice were used as positive control for Rb482 antibody. To characterize the local immune response at the entry site, the identification of macrophage populations (Mac-3) and

cells producing chemical mediators (TNF-α, IL-1α, IL-6, IL-10 and IFN-γ) was carried out on 3-$\mu$m sections of zinc salt-fixed distal small intestine samples. No epitope-retrieval treatments were needed for these antibodies. Details for primary antibodies used, including dilutions and antigen-retrieval methods, are summarized in Table 1.

Tissue sections from PrPd-inoculated animals, in which the specific primary antibodies were replaced by rabbit or mouse non-immune serum and Tris Buffer Saline-Tween 20, were used as negative controls. Samples from the non-inoculated animals and normal-brain-inoculated animals were also used as negative controls.

### *Cell counts*

The presence of reactive cells against Rb482 antibody was evaluated in one 10% formalin-fixed section of distal small intestine, mesenteric lymphnodes and brain per animal –six per timepoint – and was expressed semiquantitatively as follows: 0, none; 1, scarce; 2, moderate; 3, abundant. For Mac-3, TNF-α, IL-1α, IL-6, IL-10 and IFN-γ antibodies, one zinc salt-fixed section of distal small intestine per animal –six per timepoint – was selected and cell counts were made in 25 consecutive areas of 0.2 $mm^2$. Counts were made separately in epithelium, lamina propria/submucosa and Peyer´s patches. Cells were distinguished by virtue of their location, size and morphological features, and distribution was expressed as cells per 0.2 $mm^2$.

### *Statistical analysis*

Statistical analysis was performed with a specific software program. Data on immunopositive cells were assessed to calculate mean and standard deviation (SD). Differences between control-group values (NI, *non inoculated* and NBI, *normal brain inoculated* at 0, 35, 90 and 270 dpi respectively) and inoculated-animal values in each timepoint were tested using the unpaired t-test Welch corrected (for Gaussian distributions) and the Mann-Whitney's U-test (for non-parametric distributions). Different significance values of P were considered (*, $P<0.05$; **, $P<0.01$ and ***, $P<0.001$ for unpaired t-test and †, $P<0.05$; ††, $P<0.01$ and †††, $P<0.001$ for Mann-Whitney's-U test).

## Results

### *Clinical signs, gross lesions and morphological changes*

PrPd-infected mice showed typical signs of the disease at 270 dpi, consisting of stagger, arched back and erected tail and hair. As progression of the disease was evident at this timepoint, the remaining animals (mice originally designed to be killed at 300, 350 and 400 dpi) were sacrificed for ethical reasons between 270 and 300 dpi and sample collection was halted. No significant gross lesions were found in infected animal necropsies. Control animals showed neither clinical signs nor gross lesions throughout the experiment.

Morphological study was performed on distal small intestine samples. Significant structural changes were not observed in infected mice at any timepoint evaluated in the histopathological study. However, ultrastructural analysis revealed the presence of numerous fibrillar protein deposits, ranging between 15 and 20 nm in thickness, in enterocyte and intraepithelial macrophage cytoplasms, giving rise to a higher electrondensity of these cells (Fig. 1A-C). This finding was observed from the start of the experiment and was interpreted as a disorganization of the microtubule network. Finally, normal brain-inoculated animals (control group 1) and non-inoculated animals (control group 2) developed neither structural nor ultrastructural lesions.

### *PrPd distribution*

Immunohistochemical analysis was performed using the Rb482 antibody. Identification of the different cell types labelling to PrPd was based on morphological criteria. PrPd was detected in the form of large intracytoplasmic deposits in tingible body macrophages; these cells appeared larger than normal, with bean-shaped nuclei and abundant cytoplasm containing phagocytized cell debris (tingible bodies). Moreover, granular depositions resembling reticular structures were observed in follicular dendritic cells; these cell types were located inside lymphoid follicles displaying oval to

**Table 1.** Details of the primary antibodies used in the immunohistochemical study.

| Antibody (clone) | Antigen | Type | Dilution[c] | Antigen-retrieval method | Source |
|---|---|---|---|---|---|
| Rb482 | PrP | Po[a] | 1:2000 | Citrated autoclaving[d] | Veterinary Laboratories Agency |
| M3/84 | Mac-3 | Mo[b] | 1 :100 | None | BD Pharmingen |
| XT3 | TNF-α | Po | 1 :100 | None | Pierce Endogen |
| IL8A-H12 | IL-1α | Po | 1 :100 | None | Pierce Endogen |
| MP5-20F3 | IL-6 | Mo | 1 :100 | None | AbD Serotec |
| JES5-2A5 | IL-10 | Mo | 1 :100 | None | AbD Serotec |
| RMMG-1 | IFN-γ | Mo | 1 :100 | None | Calbiochem |

[a]: Polyclonal; [b]: Monoclonal; [c]: In Tris buffer saline-Tween 20; [d]: In 10 mM citrate buffer, pH 6.1, for 30 min at 121 ºC.

round nuclei and thick cytoplasmic projections (dendrites).

The results indicated an increase in the presence of PrPd (Fig. 1D-F) in tingible body macrophages and follicular dendritic cells within lymphoid follicles in the PPs of infected mice from 60 dpi, peaking at 180 dpi and decreasing slightly until the end of the experiment (Table 2). PrPd was also detected in tingible body macrophages

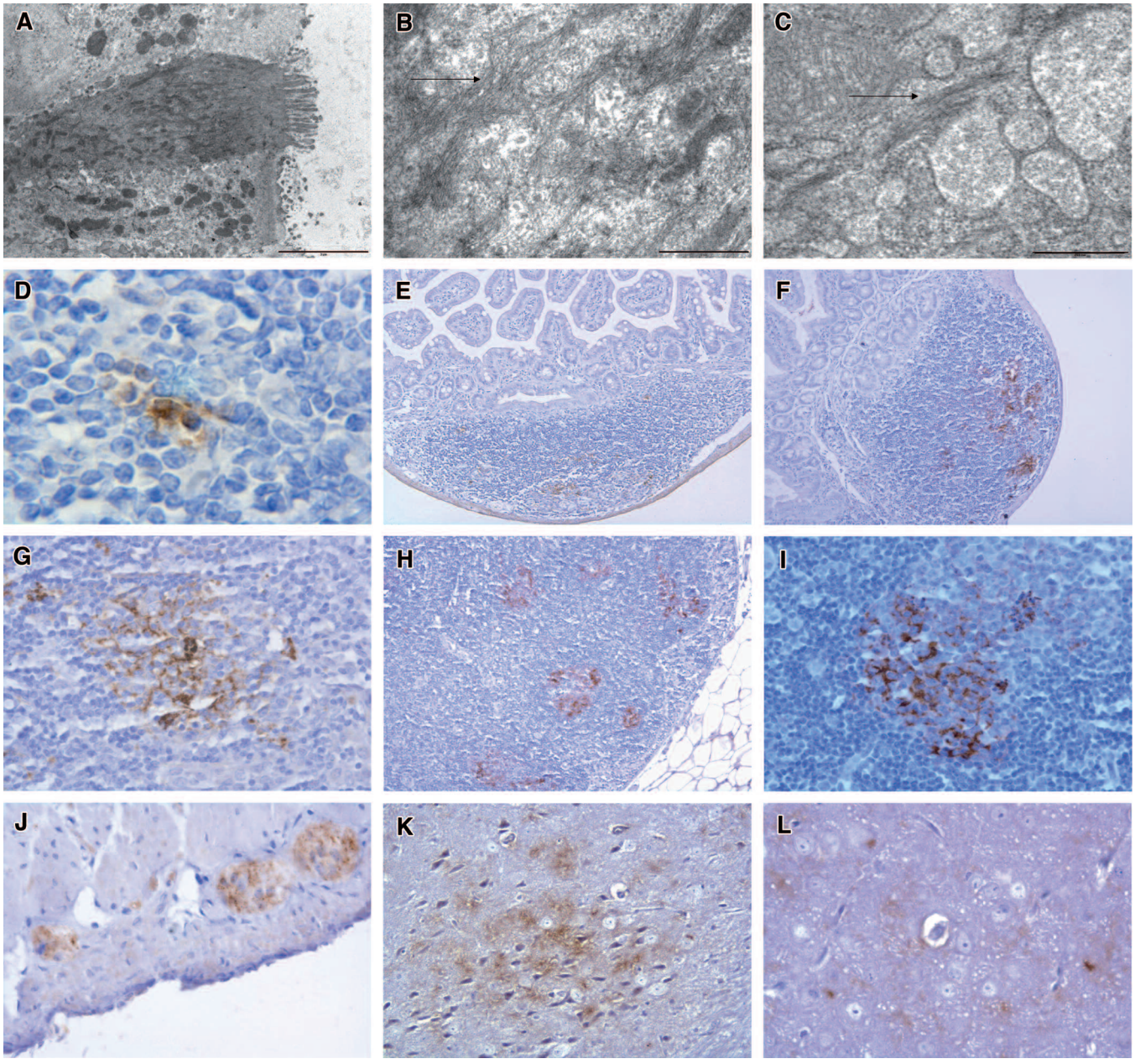


**Fig. 1.** Ultrastructural findings and immunohistochemical detection of PrPd in the different structures evaluated. **A.** Presence of abnormal fibrilar protein deposits inside an enterocyte. Note the higher electrondensity of this epithelial cell (Transmission electron microscopy (TEM), 45 dpi, Bar: 2 $\mu$m). **B.** Detail of the previous image at higher magnification. Observe the 15-20 nm thickness fibrils distributed by the cytoplasm (arrow, TEM, 45 dpi, Bar: 500 nm). **C.** Same proteins in the cytoplasm of an intraepithelial macrophage (arrow, TEM, 45 dpi, Bar: 500 nm). **D.** PrPd accumulation inside lymphoid follicle cells of PPs (Immunohistochemistry (IHC), 120 dpi, Bar: 10 $\mu$m). **E.** Positive reaction against the pathogenic prion inside PPs (IHC, 120 dpi, Bar: 100 $\mu$m). **F.** Highest detection of pathogenic prion protein in PPs (IHC, 180 dpi, Bar: 100 $\mu$m). **G**, Presence of PrPd inside lymphoid follicles of mesenteric lymphnodes (IHC, 120 dpi, Bar: 25 $\mu$m). **H**, Positive immunoreaction against PrPd in lymphoid follicles of mesenteric lymphnodes (IHC, 180 dpi, Bar: 100 $\mu$m). **I.** Detail of the highest detection of the pathogenic prion protein in a lymphoid follicle of mesenteric lymphnodes (IHC, 180 dpi, Bar: 25 $\mu$m). **J.** Myenteric nervous plexus showing immunoreactivity against PrPd (IHC, 270 dpi, Bar: 25 $\mu$m). **K.** Granular and diffuse accumulation of PrPd in the brain neuropil (IHC, 180 dpi, Bar: 50 $\mu$m). **L.** Typical pathogenic prion protein rosettes observed in the brain neuropil (IHC, 180 dpi, Bar: 25 $\mu$m).

and follicular dendritic cells located within the lymphoid follicles of mesenteric lymphnodes from 60 dpi (Fig. 1G-I). PrPd could not be demonstrated either in intestinal lymphoid aggregates or in epithelial cells. In gut myoenteric nervous plexus located between the two layers of muscular tissue, PrPd was detected as fine, punctate, intracellular aggregates from 120 dpi onwards (Fig. 1J). In brain sections, PrPd was observed as a diffuse granular deposition in the neuropil from 180 dpi (Fig. 1K,L). Typical PrPd aggregates were also found occasionally in brain tissues. Sequential distribution of PrPd in the evaluated tissues, together with the appearance of clinical signs, is summarized in Table 3. No PrPd was detected in the intestine, mesenteric lymphnodes, myoenteric nerve plexus or brain of negative control groups.

### *Changes in intestinal macrophage populations*

Mac-3 antibody recognized macrophages and dendritic cells. However, only large cells with abundant cytoplasm and vesicular nuclei, morphologically identified as macrophages, were counted.

An increase in the number of Mac-3-positive

**Table 2.** Evaluation of the PrPd presence in PPs from PrPd-inoculated animals at different timepoints.

| dpi | 15 | 35 | 45 | 60 | 75 | 90 | 105 | 120 | 150 | 180 | 210 | 240 | 270 |
|---|---|---|---|---|---|---|---|---|---|---|---|---|---|
| Positive/examined | 0/6 | 0/6 | 0/6 | 4/6 | 6/6 | 6/6 | 6/6 | 6/6 | 6/6 | 6/6 | 6/6 | 4/4[a] | 4/4[a] |
| Average intensity of PrPd deposition[b] | 0 | 0 | 0 | 1 | 1 | 1 | 1.16 | 1.5 | 1.83 | 2.16 | 1.5 | 1 | 1.25 |

[a]: PrPd presence was only examined in Peyer's patches of four animals due to the absence of this structure in sections of the other two animals from the group of sacrifice. [b]: Average intensity is shown as a mean of the presence of PrPd in individual animals, evaluated semiquantitatively as follows: 0 (none); 1 (scarce); 2 (moderate); 3 (abundant).

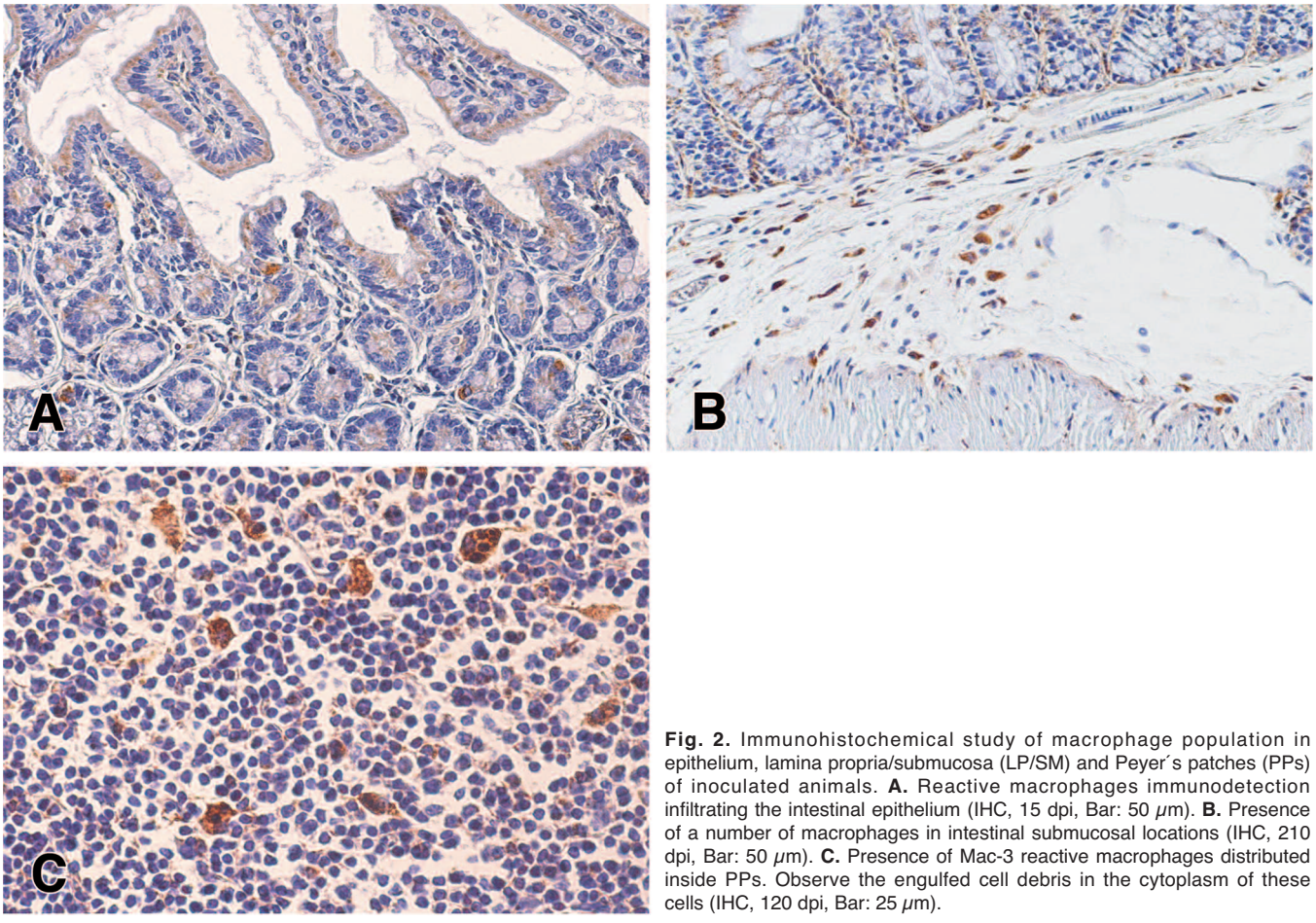


**Fig. 2.** Immunohistochemical study of macrophage population in epithelium, lamina propria/submucosa (LP/SM) and Peyer´s patches (PPs) of inoculated animals. **A.** Reactive macrophages immunodetection infiltrating the intestinal epithelium (IHC, 15 dpi, Bar: 50 $\mu$m). **B.** Presence of a number of macrophages in intestinal submucosal locations (IHC, 210 dpi, Bar: 50 $\mu$m). **C.** Presence of Mac-3 reactive macrophages distributed inside PPs. Observe the engulfed cell debris in the cytoplasm of these cells (IHC, 120 dpi, Bar: 25 $\mu$m).

intraepithelial macrophages was detected in infected animals from the start of the experiment, peaking at 15 dpi. Thenceforth, a slight and progressive decrease in the number of positive macrophages was observed until the end of the experiment. However, the number of Mac-3-positive intraepithelial macrophages remained significantly higher than in control mice until 150 dpi (Table 4, Fig. 2A).

The number of Mac-3-positive macrophages in the lamina propria/submucosa of infected mice was significantly higher than in controls throughout the experiment. Mac-3 positive macrophage numbers increased significantly from 15 dpi, peaking at 75 dpi; thereafter, a progressive decrease in numbers was

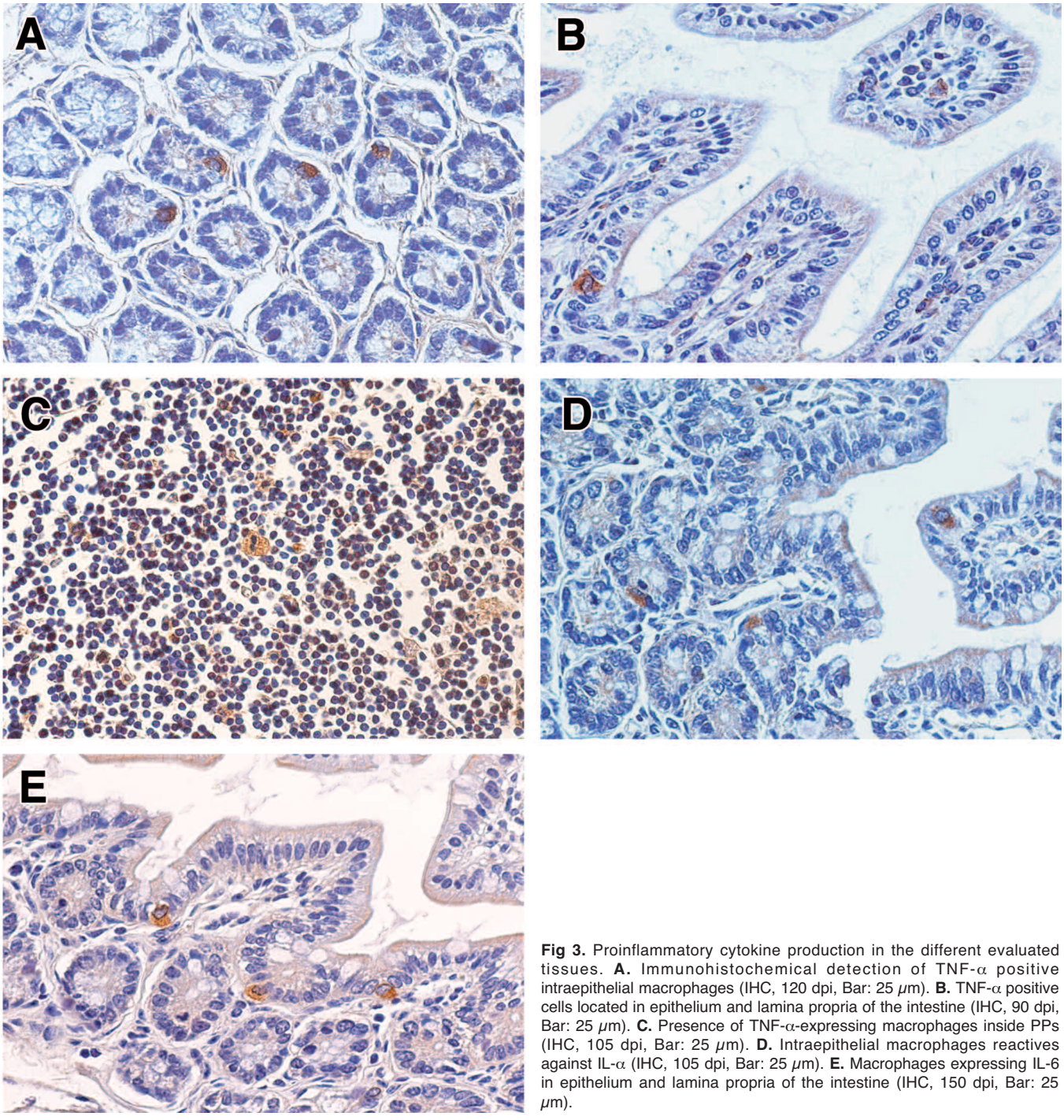


**Fig 3.** Proinflammatory cytokine production in the different evaluated tissues. **A.** Immunohistochemical detection of TNF-α positive intraepithelial macrophages (IHC, 120 dpi, Bar: 25 μm). **B.** TNF-α positive cells located in epithelium and lamina propria of the intestine (IHC, 90 dpi, Bar: 25 μm). **C.** Presence of TNF-α-expressing macrophages inside PPs (IHC, 105 dpi, Bar: 25 μm). **D.** Intraepithelial macrophages reactives against IL-α (IHC, 105 dpi, Bar: 25 μm). **E.** Macrophages expressing IL-6 in epithelium and lamina propria of the intestine (IHC, 150 dpi, Bar: 25 μm).

observed until 180 dpi (Table 4, Fig. 2B). Thenceforth, the number of positive macrophages showed a slight increase until the end of the experiment.

Finally, in PPs lymphoid follicles, changes in Mac-3-positive macrophage numbers mirrored those observed in the lamina propria/submucosa of infected mice. The number of labelled macrophages peaked at 75 dpi, decreasing gradually thereafter until 180 dpi and thereafter increasing slightly until the end of the experiment (Table 4, Fig. 2C). The number of Mac-3-positive macrophages within PPs lymphoid follicles was considerably higher than in lamina propria/submucosa throughout the experiment.

### *Cytokine dynamics in the intestine*

In order to determine whether immunocompetent cells might be involved in an inflammatory and immune

**Table 3.** Sequential detection of PrPd in the different studied areas and appearing of clinical signs.

| dpi | 0 | 15 | 35 | 45 | 60 | 75 | 90 | 105 | 120 | 150 | 180 | 210 | 240 | 270 |
|---|---|---|---|---|---|---|---|---|---|---|---|---|---|---|
| Peyer's patches | | | | | ■ | ■ | ■ | ■ | ■ | ■ | ■ | ■ | ■ | ■ |
| Mesenteric lymphnodes | | | | | ■ | ■ | ■ | ■ | ■ | ■ | ■ | ■ | ■ | ■ |
| Myenteric nervous plexus | | | | | | | | | ■ | ■ | ■ | ■ | ■ | ■ |
| Brain | | | | | | | | | | | ■ | ■ | ■ | ■ |
| Clinical signs | | | | | | | | | | | | | | ■ |

□ No detection; ■ Detection

**Table 4.** Evolution in the number of reactive macrophages in inoculated (upper line) and control animals (left column).

| Mac-3 Epithelium (Mean±SD) | | 15 dpi 1.52±0.84 | 35 dpi 1.47±0.53 | 45 dpi 0.92±0.45 | 60 dpi 0.99±0.38 | 75 dpi 1.19±0.51 | 90 dpi 0.63±0.28 | 105 dpi 0.48±0.29 | 120 dpi 0.67±0.28 | 150 dpi 0.56±0.26 | 180 dpi 0.4±0.2 | 210 dpi 0.3±0.23 | 240 dpi 0.33±0.31 | 270 dpi 0.36±0.42 |
|---|---|---|---|---|---|---|---|---|---|---|---|---|---|---|
| 0 dpi | NI (0.32±0.22) | *** | *** | *** | *** | *** | *** | * | *** | *** | ns | ns | ns | ns |
| | NBI (0.31±0.24) | *** | *** | *** | *** | *** | *** | * | *** | *** | ns | ns | ns | ns |
| 35 dpi | NI (0.35±0.25) | *** | *** | *** | *** | *** | *** | * | *** | *** | ns | ns | ns | ns |
| | NBI (0.34±0.24) | *** | *** | *** | *** | *** | *** | * | *** | *** | ns | ns | ns | ns |
| 90 dpi | NI (0.29±0.19) | *** | *** | *** | *** | *** | *** | * | *** | *** | ns | ns | ns | ns |
| | NBI (0.3±0.2) | *** | *** | *** | *** | *** | *** | * | *** | *** | ns | ns | ns | ns |
| 270 dpi | NI (0.33±0.23) | *** | *** | *** | *** | *** | *** | * | *** | *** | ns | ns | ns | ns |
| | NBI (0.35±0.25 | *** | *** | *** | *** | *** | *** | * | *** | *** | ns | ns | ns | ns |

| Mac-3 LP/SM (Mean±SD) | | 15 dpi 0.55±0.31 | 35 dpi 1.23±0.48 | 45 dpi 2.32±0.91 | 60 dpi 3.14±0.91 | 75 dpi 6.55±1.91 | 90 dpi 4.13±1.66 | 105 dpi 2.98±1.11 | 120 dpi 4.84±1.58 | 150 dpi 3.74±1.56 | 180 dpi 2.88±1.19 | 210 dpi 3.41±2.08 | 240 dpi 3.63±1.60 | 270 dpi 3.94±2.03 |
|---|---|---|---|---|---|---|---|---|---|---|---|---|---|---|
| 0 dpi | NI (0.26±0.38) | ** | *** | *** | *** | *** | *** | *** | *** | *** | *** | *** | *** | *** |
| | NBI (0.25±0.37) | ** | *** | *** | *** | *** | *** | *** | *** | *** | *** | *** | *** | *** |
| 35 dpi | NI (0.29±0.41) | ** | *** | *** | *** | *** | *** | *** | *** | *** | *** | *** | *** | *** |
| | NBI (0.28±0.4) | ** | *** | *** | *** | *** | *** | *** | *** | *** | *** | *** | *** | *** |
| 90 dpi | NI (0.23±0.35) | ** | *** | *** | *** | *** | *** | *** | *** | *** | *** | *** | *** | *** |
| | NBI (0.24±0.36) | ** | *** | *** | *** | *** | *** | *** | *** | *** | *** | *** | *** | *** |
| 270 dpi | NI (0.27±0.39) | ** | *** | *** | *** | *** | *** | *** | *** | *** | *** | *** | *** | *** |
| | NBI (0.29±0.41) | ** | *** | *** | *** | *** | *** | *** | *** | *** | *** | *** | *** | *** |

| Mac-3 PPs (Mean±SD) | | 15 dpi 8.2±8.67 | 35 dpi 19.85±8.47 | 45 dpi 9.75±5.80 | 60 dpi 17.57±14.61 | 75 dpi 32.16±13.34 | 90 dpi 25.8±10.18 | 105 dpi 27.4±11.26 | 120 dpi 27.33±5.50 | 150 dpi 22.81±9.57 | 180 dpi 19.7±9.34 | 210 dpi 23.66±16.25 | 240 dpi 21±12 | 270 dpi 22±14 |
|---|---|---|---|---|---|---|---|---|---|---|---|---|---|---|
| 0 dpi | NI (5±3) | ns | ** | *** | * | *** | ** | ** | * | *** | *** | * | * | * |
| | NBI (5±4) | ns | ** | *** | * | *** | ** | ** | * | *** | *** | * | * | * |
| 35 dpi | NI (6±4) | ns | ** | *** | * | *** | ** | ** | * | *** | *** | * | * | * |
| | NBI (4±2) | ns | ** | *** | * | *** | ** | ** | * | *** | *** | * | * | * |
| 90 dpi | NI (4±2) | ns | ** | *** | * | *** | ** | ** | * | *** | *** | * | * | * |
| | NBI (6±4) | ns | ** | *** | * | *** | ** | ** | * | *** | *** | * | * | * |
| 270 dpi | NI (4±2) | ns | ** | *** | * | *** | ** | ** | * | *** | *** | * | * | * |
| | NBI (6±4) | ns | ** | *** | * | *** | ** | ** | * | *** | *** | * | * | * |

Differences from controls (NI, non inoculated and NBI, normal brain inoculated at 0, 35, 90 and 270 dpi) were considered statistically significant (*: P<0.05; **: P<0.01; and ***: P<0.001 for student-t test or †, P<0.05; ††, P<0.01; and †††, P<0.001 from Mann-Whitney's-U test).

**Table 5.** Evolution in the number of reactive cells against TNF-α in inoculated (upper line) and control animals (left column).

| TNF-α Epithelium (Mean±SD) | | 15 dpi 1.84±0.68 | 35 dpi 1.32±0.62 | 45 dpi 1.45±0.64 | 60 dpi 0.4±0.36 | 75 dpi 0.85±0.43 | 90 dpi 0.94±0.43 | 105 dpi 1.56±0.81 | 120 dpi 1.44±0.63 | 150 dpi 1.72±0.61 | 180 dpi 1.36±0.49 | 210 dpi 1.98±0.67 | 240 dpi 1.81±0.64 | 270 dpi 1.72±1.13 |
|---|---|---|---|---|---|---|---|---|---|---|---|---|---|---|
| 0 dpi | NI (1.32±0.69) | ** | ns | ns | *** | ** | * | ns | ns | * | ns | ** | * | ns |
| | NBI (1.33±0.71) | ** | ns | ns | *** | ** | * | ns | ns | * | ns | ** | * | ns |
| 35 dpi | NI (1.35±0.72) | ** | ns | ns | *** | ** | * | ns | ns | * | ns | ** | * | ns |
| | NBI (1.34±0.71) | ** | ns | ns | *** | ** | * | ns | ns | * | ns | ** | * | ns |
| 90 dpi | NI (1.29±0.66) | ** | ns | ns | *** | ** | * | ns | ns | * | ns | ** | * | ns |
| | NBI (1.3±0.67) | ** | ns | ns | *** | ** | * | ns | ns | * | ns | ** | * | ns |
| 270 dpi | NI (1.33±0.7) | ** | ns | ns | *** | ** | * | ns | ns | * | ns | ** | * | ns |
| | NBI (1.35±0.72) | ** | ns | ns | *** | ** | * | ns | ns | * | ns | ** | * | ns |
| TNF-α LP/SM (Mean±SD) | | 15 dpi 1.59±0.5 | 35 dpi 1.19±0.45 | 45 dpi 1.03±0.57 | 60 dpi 0.33±0.32 | 75 dpi 0.71±0.29 | 90 dpi 1.08±0.46 | 105 dpi 1.29±0.41 | 120 dpi 1.12±0.59 | 150 dpi 1.68±0.58 | 180 dpi 1.13±0.6 | 210 dpi 1.1±0.44 | 240 dpi 1.22±0.66 | 270 dpi 1.4±1.15 |
| 0 dpi | NI (1.52±0.85) | ns | ns | * | *** | *** | * | ns | ns | ns | ns | * | ns | ns |
| | NBI (1.53±0.85) | ns | ns | * | *** | *** | * | ns | ns | ns | ns | * | ns | ns |
| 35 dpi | NI (1.55±0.88) | ns | ns | * | *** | *** | * | ns | ns | ns | ns | * | ns | ns |
| | NBI (1.54±0.87) | ns | ns | * | *** | *** | * | ns | ns | ns | ns | * | ns | ns |
| 90 dpi | NI (1.49±0.82) | ns | ns | * | *** | *** | * | ns | ns | ns | ns | * | ns | ns |
| | NBI (1.5±0.83) | ns | ns | * | *** | *** | * | ns | ns | ns | ns | * | ns | ns |
| 270 dpi | NI (1.53±0.86) | ns | ns | * | *** | *** | * | ns | ns | ns | ns | * | ns | ns |
| | NBI (1.55±0.88) | ns | ns | * | *** | *** | * | ns | ns | ns | ns | * | ns | ns |
| TNF-α PPs (Mean±SD) | | 15 dpi 0.25±0.5 | 35 dpi 0±0 | 45 dpi 0±0 | 60 dpi 0±0 | 75 dpi 0±0 | 90 dpi 0.3±0.67 | 105 dpi 0.6±1.34 | 120 dpi 0.25±0.5 | 150 dpi 0.33±0.81 | 180 dpi 0±0 | 210 dpi 0±0 | 240 dpi 0.12±0.25 | 270 dpi 0.25±0.5 |
| 0 dpi | NI (0.12±0.25) | ns | ns | ns | ns | ns | † | † | ns | † | ns | ns | ns | ns |
| | NBI (0.13±0.28) | ns | ns | ns | ns | ns | † | † | ns | † | ns | ns | ns | ns |
| 35 dpi | NI (0.15±0.28) | ns | ns | ns | ns | ns | † | † | ns | † | ns | ns | ns | ns |
| | NBI (0.14±0.27) | ns | ns | ns | ns | ns | † | † | ns | † | ns | ns | ns | ns |
| 90 dpi | NI (0.09±0.22) | ns | ns | ns | ns | ns | † | † | ns | † | ns | ns | ns | ns |
| | NBI (0.1±0.23) | ns | ns | ns | ns | ns | † | † | ns | † | ns | ns | ns | ns |
| 270 dpi | NI (0.13±0.26) | ns | ns | ns | ns | ns | † | † | ns | † | ns | ns | ns | ns |
| | NBI (0.15±0.28) | ns | ns | ns | ns | ns | † | † | ns | † | ns | ns | ns | ns |

Differences from controls (NI, non inoculated and NBI, normal brain inoculated at 0, 35, 90 and 270 dpi) were considered statistically significant (*: P<0.05; **: P<0.01; and ***: P<0.001 for student-t test or †, P<0.05; ††, P<0.01; and †††, P<0.001 from Mann-Whitney's-U test).

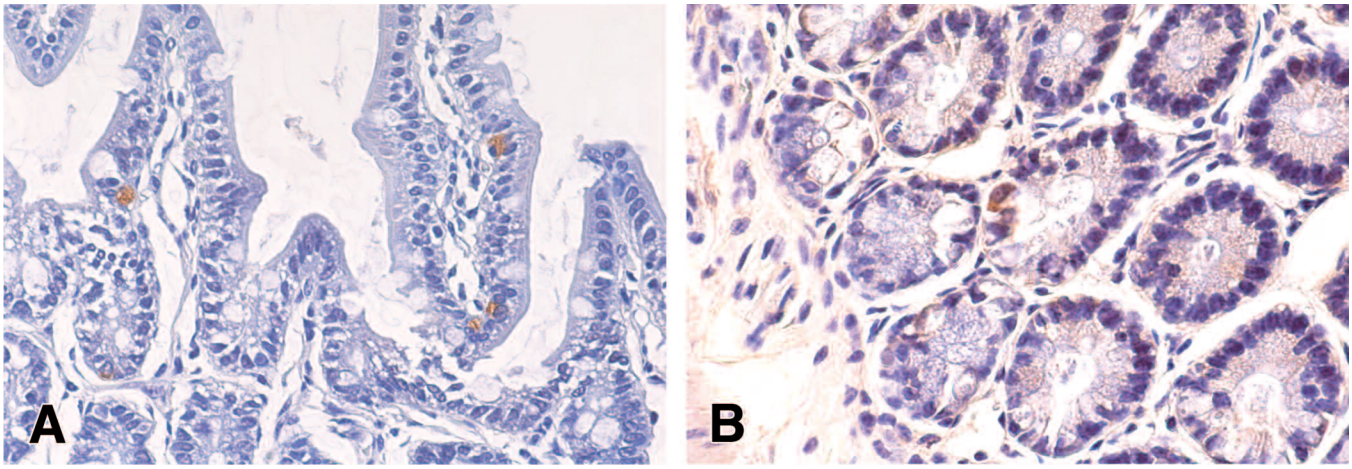


**Fig. 4.** Production of cytokines related with Th1/Th2 immune response in the structures studied. **A.** Presence of positive immunoreaction in intraepithelial cells against IL-10 (IHC, 150 dpi, Bar: 25 μm). **B.** IFN-γ expressing-cell infiltrated in the epithelium (IHC, 180 dpi, Bar: 25 μm).

response against PrPd at natural entry sites, cytokines with proinflammatory activity (TNF-α, IL-1α and IL-6) as well as other cytokines (IFN-γ and IL-10) involved in the cell-mediated immune response (Th1-Th2) were evaluated by immunohistochemical methods.

a) Proinflammatory cytokines

TNF-α was the main cytokine detected in cells located in the epithelium and lamina propria/submucosa of infected animals, whereas IL-1α was the main cytokine observed in mononuclear cells within PPs lymphoid follicles.

TNF-α-positive cells were mainly identified as macrophages, although some positive lymphocytes were occasionally observed. Changes in the number of positive cells in epithelium and lamina propria/submucosa were similar throughout the experiment. The number of intraepithelial macrophages producing TNF-α displayed a significant increase with respect to controls at 15 dpi. Thereafter the number of cells producing this cytokine decreased gradually in the epithelium as well as in the lamina propria/submucosa, with numbers significantly lower than those of controls between 45 and 90 dpi. The number of TNF-α positive cells in these areas reached the lowest levels at 60 dpi (Table 5. Fig. 3A,B). From 105 dpi onwards, there was a progressive increase in the number of positive cells. However, in the lamina propria/submucosa, the number of TNF-α positive cells was lower than, or similar to, that recorded in control mice, while in the epithelium the presence of TNF-α positive cells was significantly higher than in controls during the final stage of the experiment (210-240 dpi). Production of TNF-α in PPs lymphoid follicles was very scarce throughout the experiment (Table 5, Fig. 3C). No expression of this cytokine was observed between 35 and 75 dpi or between 180 and 210 dpi, values being significantly lower than in controls.

The number of IL-1α positive cells, mainly macrophages, was scarce in epithelium and lamina propria/submucosa from disease onset. These cells displayed significantly lower values than controls between 35 and 90 dpi and from 150 dpi to the end of the experiment (Table 6; Fig. 3D). However, in PPs

**Table 6.** Evolution in the number of reactive cells against IL-1α in inoculated (upper line) and control animals (left column).

| IL-1α Epithelium (Mean±SD) | | 15 dpi 0.84±0.45 | 35 dpi 0.33±0.22 | 45 dpi 0.65±0.47 | 60 dpi 0.4±0.4 | 75 dpi 0.81±0.36 | 90 dpi 0.54±0.31 | 105 dpi 0.69±0.37 | 120 dpi 0.74±0.55 | 150 dpi 0.38±0.34 | 180 dpi 0.36±0.34 | 210 dpi 0.3±0.29 | 240 dpi 0.27±0.27 | 270 dpi 0.28±0.45 |
|---|---|---|---|---|---|---|---|---|---|---|---|---|---|---|
| 0 dpi | NI (0.78±0.39) | ns | *** | ns | ** | ns | * | ns | ns | *** | *** | *** | *** | *** |
| | NBI (0.79±0.4) | ns | *** | ns | ** | ns | * | ns | ns | *** | *** | *** | *** | *** |
| 35 dpi | NI (0.81±0.42) | ns | *** | ns | ** | ns | * | ns | ns | *** | *** | *** | *** | *** |
| | NBI (0.8±0.41) | ns | *** | ns | ** | ns | * | ns | ns | *** | *** | *** | *** | *** |
| 90 dpi | NI (0.75±0.36) | ns | *** | ns | ** | ns | * | ns | ns | *** | *** | *** | *** | *** |
| | NBI (0.76±0.37) | ns | *** | ns | ** | ns | * | ns | ns | *** | *** | *** | *** | *** |
| 270 dpi | NI (0.79±0.4) | ns | *** | ns | ** | ns | * | ns | ns | *** | *** | *** | *** | *** |
| | NBI (0.81±0.42) | ns | *** | ns | ** | ns | * | ns | ns | *** | *** | *** | *** | *** |

| IL-1α LP/SM (Mean±SD) | | 15 dpi 0.83±0.41 | 35 dpi 0.35±0.2 | 45 dpi 0.42±0.35 | 60 dpi 0.35±0.34 | 75 dpi 0.4±0.29 | 90 dpi 0.41±0.3 | 105 dpi 0.67±0.33 | 120 dpi 0.44±0.29 | 150 dpi 0.56±0.32 | 180 dpi 0.56±0.31 | 210 dpi 0.16±0.28 | 240 dpi 0.19±0.26 | 270 dpi 0.24±0.52 |
|---|---|---|---|---|---|---|---|---|---|---|---|---|---|---|
| 0 dpi | NI (0.8±0.37) | ns | *** | *** | *** | *** | *** | ns | *** | * | * | *** | *** | *** |
| | NBI (0.79±0.38) | ns | *** | *** | *** | *** | *** | ns | *** | * | * | *** | *** | *** |
| 35 dpi | NI (0.81±0.42) | ns | *** | *** | *** | *** | *** | ns | *** | * | * | *** | *** | *** |
| | NBI (0.8±0.41) | ns | *** | *** | *** | *** | *** | ns | *** | * | * | *** | *** | *** |
| 90 dpi | NI (0.75±0.36) | ns | *** | *** | *** | *** | *** | ns | *** | * | * | *** | *** | *** |
| | NBI (0.76±0.37) | ns | *** | *** | *** | *** | *** | ns | *** | * | * | *** | *** | *** |
| 270 dpi | NI (0.79±0.4) | ns | *** | *** | *** | *** | *** | ns | *** | * | * | *** | *** | *** |
| | NBI (0.81±0.42) | ns | *** | *** | *** | *** | *** | ns | *** | * | * | *** | *** | *** |

| IL-1α PPs (Mean±SD) | | 15 dpi 0.25±0.5 | 35 dpi 1±2.44 | 45 dpi 0±0 | 60 dpi 0±0 | 75 dpi 0.36±0.92 | 90 dpi 1.33±3.31 | 105 dpi 0.25±0.46 | 120 dpi 0.66±1.15 | 150 dpi 0.6±1.34 | 180 dpi 0.08±0.28 | 210 dpi 0±0 | 240 dpi 0±0 | 270 dpi 0±0 |
|---|---|---|---|---|---|---|---|---|---|---|---|---|---|---|
| 0 dpi | NI (0±0) | † | † | ns | ns | † | † | † | † | † | ns | ns | ns | ns |
| | NBI (0±0) | † | † | ns | ns | † | † | † | † | † | ns | ns | ns | ns |
| 35 dpi | NI (0±0) | † | † | ns | ns | † | † | † | † | † | ns | ns | ns | ns |
| | NBI (0±0) | † | † | ns | ns | † | † | † | † | † | ns | ns | ns | ns |
| 90 dpi | NI (0±0) | † | † | ns | ns | † | † | † | † | † | ns | ns | ns | ns |
| | NBI (0±0) | † | † | ns | ns | † | † | † | † | † | ns | ns | ns | ns |
| 270 dpi | NI (0±0) | † | † | ns | ns | † | † | † | † | † | ns | ns | ns | ns |
| | NBI (0±0) | † | † | ns | ns | † | † | † | † | † | ns | ns | ns | ns |

Differences from controls (NI, non inoculated and NBI, normal brain inoculated at 0, 35, 90 and 270 dpi) were considered statistically significant (*: P<0.05; **: P<0.01; and ***: P<0.001 for student-t test or †, P<0.05; ††, P<0.01; and †††, P<0.001 from Mann-Whitney's-U test).

lymphoid follicles there was a significant increase in IL-1α production during the initial stages (15 and 35 dpi), followed by an absence of reactive cells between 45 and 60 dpi and by a significant increase from 75 to 150 dpi.

The presence of IL-6 positive cells (mainly macrophages) in epithelium and lamina propria/submucosa was also scarce from the start of the experiment. Positive-cell numbers were similar to, or significantly lower than, those recorded in control animals between 15 at 90 dpi (Table 7; Fig. 3E). However, from 105 dpi, a significant increase in positive cell numbers was detected, lasting until the end of the experiment. In PPs lymphoid follicles, numbers were significantly lower than in controls from 15 dpi onwards, reaching minimum levels at 35, 60, 150 and 210 dpi.

b) Th1/Th2 immune response-associated cytokines

The presence of IFN-γ -cytokine immunolabelled cells, mainly produced by T-lymphocytes during the Th1 immune response, and of IL-10 produced during the Th2 immune response, was scarce in epithelium and lamina propria/submucosa (Tables 8, 9; Fig. 4A,B). A significant increase in IFN-γ production was noted in these locations during the initial stages of the experiment, together with a significant drop in the number of IL-10 positive cells between 15 and 90 dpi.

From 15 dpi until the end of the experiment, a progressive decrease in the number of IFN-Á positive cells was observed within PPs lymphoid follicles, numbers being significantly lower than those recorded in controls. The presence of IFN-γ positive cells reached minimum levels between 105 and 120 dpi, when no reactive cells were detected. Moreover, the presence of IL-10 positive cells in PP lymphoid follicles had significantly lower values than in controls throughout the experiment.

## Discussion

The results obtained here suggest that macrophages may play a role in the uptake and transport of PrPd from the intestinal lumen to underlying lymphoid tissues following experimental oral inoculation. Furthermore, there may be an early impairment of the local immune response, as a result of which the inhibition of

**Table 7.** Evolution in the number of reactive cells against IL-6 in inoculated (upper line) and control animals (left column).

| IL-6 Epithelium (Mean±SD) | | 15 dpi 0.15±0.16 | 35 dpi 0.1±0.14 | 45 dpi 0.42±0.26 | 60 dpi 0.29±0.24 | 75 dpi 0.2±0.2 | 90 dpi 0.4±0.35 | 105 dpi 1.04±0.75 | 120 dpi 0.82±0.45 | 150 dpi 0.89±0.38 | 180 dpi 0.47±0.27 | 210 dpi 0.7±0.75 | 240 dpi 0.51±0.39 | 270 dpi 0.44±0.5 |
|---|---|---|---|---|---|---|---|---|---|---|---|---|---|---|
| 0 dpi | NI (0.31±0.2) | ** | *** | ns | ns | * | ns | *** | *** | *** | * | * | * | ns |
| | NBI (0.33±0.23) | ** | *** | ns | ns | * | ns | *** | *** | *** | * | * | * | ns |
| 35 dpi | NI (0.35±0.25) | ** | *** | ns | ns | * | ns | *** | *** | *** | * | * | * | ns |
| | NBI (0.34±0.24) | ** | *** | ns | ns | * | ns | *** | *** | *** | * | * | * | ns |
| 90 dpi | NI (0.29±0.19) | ** | *** | ns | ns | * | ns | *** | *** | *** | * | * | * | ns |
| | NBI (0.3±0.2) | ** | *** | ns | ns | * | ns | *** | *** | *** | * | * | * | ns |
| 270 dpi | NI (0.33±0.23) | ** | *** | ns | ns | * | ns | *** | *** | *** | * | * | * | ns |
| | NBI (0.35±0.25) | ** | *** | ns | ns | * | ns | *** | *** | *** | * | * | * | ns |
| IL-6 LP/SM (Mean±SD) | | 15 dpi 0.41±0.34 | 35 dpi 0.22±0.19 | 45 dpi 0.53±0.32 | 60 dpi 0.52±0.36 | 75 dpi 0.44±0.3 | 90 dpi 0.59±0.35 | 105 dpi 1.36±0.46 | 120 dpi 0.97±0.51 | 150 dpi 1.45±0.6 | 180 dpi 0.72±0.35 | 210 dpi 1.05±0.63 | 240 dpi 0.92±0.43 | 270 dpi 0.86±0.68 |
| 0 dpi | NI (0.52±0.28) | ns | *** | ns | ns | ns | ns | *** | *** | *** | * | *** | *** | * |
| | NBI (0.52±0.27) | ns | *** | ns | ns | ns | ns | *** | *** | *** | * | *** | *** | * |
| 35 dpi | NI (0.55±0.31) | ns | *** | ns | ns | ns | ns | *** | *** | *** | * | *** | *** | * |
| | NBI (0.54±0.3) | ns | *** | ns | ns | ns | ns | *** | *** | *** | * | *** | *** | * |
| 90 dpi | NI (0.49±0.25) | ns | *** | ns | ns | ns | ns | *** | *** | *** | * | *** | *** | * |
| | NBI (0.5±0.26) | ns | *** | ns | ns | ns | ns | *** | *** | *** | * | *** | *** | * |
| 270 dpi | NI (0.53±0.29) | ns | *** | ns | ns | ns | ns | *** | *** | *** | * | *** | *** | * |
| | NBI (0.55±0.31) | ns | *** | ns | ns | ns | ns | *** | *** | *** | * | *** | *** | * |
| IL-6 PPs (Mean±SD) | | 15 dpi 1±1.73 | 35 dpi 0±0 | 45 dpi 0.83±2.04 | 60 dpi 0±0 | 75 dpi 0.88±1.83 | 90 dpi 1.5±2.17 | 105 dpi 1.23±1.23 | 120 dpi 1.11±1.26 | 150 dpi 0.16±0.57 | 180 dpi 0.5±0.96 | 210 dpi 0±0 | 240 dpi 1±1.4 | 270 dpi 2±2.91 |
| 0 dpi | NI (2±2) | † | † | † | ns | † | † | † | † | † | † | † | † | ns |
| | NBI (2±2) | † | † | † | ns | † | † | † | † | † | † | † | † | ns |
| 35 dpi | NI (3±3) | † | † | † | ns | † | † | † | † | † | † | † | † | ns |
| | NBI (3±3) | † | † | † | ns | † | † | † | † | † | † | † | † | ns |
| 90 dpi | NI (1±1) | † | † | † | ns | † | † | † | † | † | † | † | † | ns |
| | NBI (2±2) | † | † | † | ns | † | † | † | † | † | † | † | † | ns |
| 270 dpi | NI (2±2) | † | † | † | ns | † | † | † | † | † | † | † | † | ns |
| | NBI (3±3) | † | † | † | ns | † | † | † | † | † | † | † | † | ns |

Differences from controls (NI, non inoculated and NBI, normal brain inoculated at 0, 35, 90 and 270 dpi) were considered statistically significant (*: P<0.05; **: P<0.01; and ***: P<0.001 for student-t test or †, P<0.05; ††, P<0.01; and †††, P<0.001 from Mann-Whitney's-U test).

macrophages, immunocompetent cells with an important role in inflammatory processes and in the immune response, together with an alteration in the production of cytokines involved in the modulation of these changes, might impede the development of a specific local immune response, favouring the accumulation and subsequent spread of PrPd.

The mechanisms involved in the uptake and transport of PrPd between intestinal wall structures and lymphoid tissue have not been yet elucidated. Some authors suggest that M cells may be involved in the uptake of PrPd from the intestinal lumen (Beekes and McBride, 2000; Heppner et al., 2001). Others report that this protein is endocytosed by enterocytes, either via the laminin receptor (Gauczynski et al., 2001) or via other cotransport mechanisms (Mishra et al., 2004). For these authors, the role of macrophages in these processes is likely to be negligible. However, the fact that the number of Mac-3-positive intraepithelial macrophages peaked at early stages of the disease (15 dpi), and that a disorganization of the microtubule network was observed in macrophage cytoplasms from the initial stages of the experiment – a finding also observed by other authors (Nieznanski et al., 2006) – would support the hypothesis that macrophages may play a role in the transport of PrPd to PPs. In addition, the presence of similar protein deposits in enterocytes suggests that these cells may also be involved in PrPd internalization. This hypothesis is further borne out by immunohistochemical demonstration of the presence of PrPd in enterocytes (Bons et al., 1999) and supports the notion that gastrointestinal tract epithelial cells may represent a possible target for prion entry and replication (Pammer et al., 2000). Furthermore, the fact that enterocytes may destroy material luminal uptaken material in phagolysosomes, together with the ability of macrophages to destroy small amounts of PrPd (Brun et al., 2003; Maignien et al., 2005), would account for both the infectious dose and the subsequent kinetics of the infection, as well as explaining the individual variations observed between different animals. Recent studies have demonstrated that PrPd is readily digested by alimentary tract fluids in sheep (Jeffrey et al., 2006) and that animals could shed a small amount of the perorally inoculated PrPd in the faeces (Krüger et al., 2009). Both mechanisms could also contribute to individual

**Table 8.** Evolution in the number of reactive cells against IL-10 in inoculated (upper line) and control animals (left column).

| IL-10 Epithelium (Mean±SD) | | 15 dpi 0.16±0.17 | 35 dpi 0.25±0.28 | 45 dpi 0.39±0.24 | 60 dpi 0.16±0.16 | 75 dpi 0.12±0.16 | 90 dpi 0.3±0.27 | 105 dpi 0.47±0.37 | 120 dpi 0.5±0.34 | 150 dpi 0.52±0.27 | 180 dpi 0.47±0.32 | 210 dpi 0.17±0.17 | 240 dpi 0.26±0.29 | 270 dpi 0.4±0.59 |
|---|---|---|---|---|---|---|---|---|---|---|---|---|---|---|
| 0 dpi | NI (0.34±0.27) | ** | ns | ns | ** | ** | ns | ns | ns | * | ns | * | ns | ns |
| | NBI (0.34±0.28) | ** | ns | ns | ** | ** | ns | ns | ns | * | ns | * | ns | ns |
| 35 dpi | NI (0.35±0.25) | ** | ns | ns | ** | ** | ns | ns | ns | * | ns | * | ns | ns |
| | NBI (0.34±0.24) | ** | ns | ns | ** | ** | ns | ns | ns | * | ns | * | ns | ns |
| 90 dpi | NI (0.29±0.19) | ** | ns | ns | ** | ** | ns | ns | ns | * | ns | * | ns | ns |
| | NBI (0.3±0.2) | ** | ns | ns | ** | ** | ns | ns | ns | * | ns | * | ns | ns |
| 270 dpi | NI (0.33±0.23) | ** | ns | ns | ** | ** | ns | ns | ns | * | ns | * | ns | ns |
| | NBI (0.35±0.25) | ** | ns | ns | ** | ** | ns | ns | ns | * | ns | * | ns | ns |
| **IL-10 LP/SM (Mean±SD)** | | **15 dpi 0.53±0.3** | **35 dpi 0.45±0.28** | **45 dpi 0.51±0.36** | **60 dpi 0.39±0.32** | **75 dpi 0.24±0.2** | **90 dpi 0.5±0.3** | **105 dpi 0.58±0.29** | **120 dpi 0.56±0.33** | **150 dpi 0.87±0.47** | **180 dpi 0.48±0.4** | **210 dpi 0.43±0.3** | **240 dpi 0.35±0.23** | **270 dpi 0.32±0.4** |
| 0 dpi | NI (0.68±0.34) | ns | * | ns | ** | *** | * | ns | ns | ns | ns | ** | *** | ** |
| | NBI (0.67±0.32) | ns | * | ns | ** | *** | * | ns | ns | ns | ns | ** | *** | ** |
| 35 dpi | NI (0.71±0.37) | ns | * | ns | ** | *** | * | ns | ns | ns | ns | ** | *** | ** |
| | NBI (0.7±0.36) | ns | * | ns | ** | *** | * | ns | ns | ns | ns | ** | *** | ** |
| 90 dpi | NI (0.65±0.31) | ns | * | ns | ** | *** | * | ns | ns | ns | ns | ** | *** | ** |
| | NBI (0.66±0.32) | ns | * | ns | ** | *** | * | ns | ns | ns | ns | ** | *** | ** |
| 270 dpi | NI (0.69±0.35) | ns | * | ns | ** | *** | * | ns | ns | ns | ns | ** | *** | ** |
| | NBI (0.69±0.35) | ns | * | ns | ** | *** | * | ns | ns | ns | ns | ** | *** | ** |
| **IL-10 PPs (Mean±SD)** | | **15 dpi 0±0** | **35 dpi 0.08±0.28** | **45 dpi 0.12±0.34** | **60 dpi 0±0** | **75 dpi 0±0** | **90 dpi 0±0** | **105 dpi 0±0** | **120 dpi 0.2±0.44** | **150 dpi 0.08±0.28** | **180 dpi 0±0** | **210 dpi 0±0** | **240 dpi 0.12±0.25** | **270 dpi 0.25±0.5** |
| 0 dpi | NI (0.64±1.33) | ns | † | † | ns | ns | ns | ns | † | † | ns | ns | † | † |
| | NBI (0.65±1.32) | ns | † | † | ns | ns | ns | ns | † | † | ns | ns | † | † |
| 35 dpi | NI (0.67±1.36) | ns | † | † | ns | ns | ns | ns | † | † | ns | ns | † | † |
| | NBI (0.66±1.35) | ns | † | † | ns | ns | ns | ns | † | † | ns | ns | † | † |
| 90 dpi | NI (0.61±1.3) | ns | † | † | ns | ns | ns | ns | † | † | ns | ns | † | † |
| | NBI (0.62±1.31) | ns | † | † | ns | ns | ns | ns | † | † | ns | ns | † | † |
| 270 dpi | NI (0.65±1.34) | ns | † | † | ns | ns | ns | ns | † | † | ns | ns | † | † |
| | NBI (0.67±1.36) | ns | † | † | ns | ns | ns | ns | † | † | ns | ns | † | † |

Differences from controls (NI, non inoculated and NBI, normal brain inoculated at 0, 35, 90 and 270 dpi) were considered statistically significant (*: P<0.05; **: P<0.01; and ***: P<0.001 for student-t test or †, P<0.05; ††, P<0.01; and †††, P<0.001 from Mann-Whitney's-U test).

variations and to infection kinetics.

From 60 dpi, accumulation of PrPd was observed in phagocytic and antigen-presenting cells in PPs, together with an increase in the number of Mac-3-positive macrophages within these lymphoid structures, which peaked at 75 dpi. There is thus a clear spatial and temporal link between the presence of PrPd and changes in the number of macrophages in the intestinal structures studied, suggesting that macrophages may be involved in the spread of PrPd from intestinal epithelium to lymphoid tissue. A number of authors have suggested that some follicular dendritic cells may in fact be migratory dendritic cells, which play a fundamental role in the transport and accumulation of PrPd from the intestinal lumen to lymphoid tissues (Huang et al., 2002; Beekes and McBride, 2007; Glaysher and Mabbott, 2007; Raymond et al., 2007); however, these studies evaluated neither the migratory capacity of macrophages nor their potential role in the spread of the pathogenic agent. The results obtained here do not rule out the role of migratory dendritic cells in the uptake and transport of the PrPd, but point to macrophages as an additional participant in these processes.

Macrophages may have been recruited initially to destroy the PrPd as part of the innate local immune response (Brun et al., 2003; Maignien et al., 2005); this mechanism would be similar in nature to the chemoattraction of migratory dendritic cells by certain prion protein fragments (Kaneider et al., 2003) and might supply a means of transporting PrPd throughout the organism. This hypothesis was borne out here by the progressive decrease observed in the number of Mac-3-positive macrophages in the structures studied from the initial stages of the experiment until 180 dpi. At this timepoint, PrPd accumulation in follicular dendritic cells and tingible body macrophages in PPs had already peaked. Thus, the decrease in the number of macrophages could point to a failed attempt by macrophages to control the replication of the pathogenic prion, enabling the subsequent spread of the PrPd to other organs.

Few studies have addressed the immune response in TSEs, since it has long been accepted that these diseases do not display the immune response typical of other

**Table 9.** Evolution in the number of positive cells against IFN-γ in inoculated (upper line) and control animals (left column).

| IFN-γ Epithelium (Mean±SD) | | 15 dpi 0.1±0.15 | 35 dpi 0.14±0.23 | 45 dpi 0.04±0.1 | 60 dpi 0.07±0.14 | 75 dpi 0.06±0.11 | 90 dpi 0.06±0.08 | 105 dpi 0.17±0.18 | 120 dpi 0.06±0.12 | 150 dpi 0.05±0.1 | 180 dpi 0.05±0.1 | 210 dpi 0.16±0.24 | 240 dpi 0.08±0.14 | 270 dpi 0.02±0.1 |
|---|---|---|---|---|---|---|---|---|---|---|---|---|---|---|
| 0 dpi | NI (0.01±0.05) | †† | †† | ns | ns | ns | † | †† | ns | ns | ns | ns | ns | ns |
| | NBI (0.01±0.05) | †† | †† | ns | ns | ns | † | †† | ns | ns | ns | ns | ns | ns |
| 35 dpi | NI (0.01±0.05) | †† | †† | ns | ns | ns | † | †† | ns | ns | ns | ns | ns | ns |
| | NBI (0.01±0.05) | †† | †† | ns | ns | ns | † | †† | ns | ns | ns | ns | ns | ns |
| 90 dpi | NI (0.01±0.05) | †† | †† | ns | ns | ns | † | †† | ns | ns | ns | ns | ns | ns |
| | NBI (0.01±0.05) | †† | †† | ns | ns | ns | † | †† | ns | ns | ns | ns | ns | ns |
| 270 dpi | NI (0.01±0.05) | †† | †† | ns | ns | ns | † | †† | ns | ns | ns | ns | ns | ns |
| | NBI (0.01±0.05) | †† | †† | ns | ns | ns | † | †† | ns | ns | ns | ns | ns | ns |
| IFN-γ LP/SM (Mean±SD) | | 15 dpi 0.18±0.18 | 35 dpi 0.15±0.15 | 45 dpi 0.08±0.14 | 60 dpi 0.13±0.18 | 75 dpi 0.06±0.09 | 90 dpi 0.1±0.13 | 105 dpi 0.17±0.27 | 120 dpi 0.16±0.24 | 150 dpi 0.06±0.14 | 180 dpi 0.08±0.11 | 210 dpi 0.26±0.36 | 240 dpi 0.08±0.14 | 270 dpi 0.04±0.13 |
| 0 dpi | NI (0.04±0.08) | †† | †† | ns | ns | ns | ns | ns | ns | ns | ns | †† | ns | ns |
| | NBI (0.05±0.1) | †† | †† | ns | ns | ns | ns | ns | ns | ns | ns | †† | ns | ns |
| 35 dpi | NI (0.05±0.09) | †† | †† | ns | ns | ns | ns | ns | ns | ns | ns | †† | ns | ns |
| | NBI (0.05±0.1) | †† | †† | ns | ns | ns | ns | ns | ns | ns | ns | †† | ns | ns |
| 90 dpi | NI (0.04±0.08) | †† | †† | ns | ns | ns | ns | ns | ns | ns | ns | †† | ns | ns |
| | NBI (0.04±0.06) | †† | †† | ns | ns | ns | ns | ns | ns | ns | ns | †† | ns | ns |
| 270 dpi | NI (0.05±0.08) | †† | †† | ns | ns | ns | ns | ns | ns | ns | ns | †† | ns | ns |
| | NBI (0.05±0.1) | †† | †† | ns | ns | ns | ns | ns | ns | ns | ns | †† | ns | ns |
| IFN-γ PPs (Mean±SD) | | 15 dpi 0.66±0.57 | 35 dpi 2.18±2.31 | 45 dpi 1.33±2.38 | 60 dpi 0.6±1.26 | 75 dpi 0.07±0.27 | 90 dpi 1.11±1.45 | 105 dpi 0±0 | 120 dpi 0±0 | 150 dpi 0.81±0.87 | 180 dpi 0.52±0.87 | 210 dpi 1.33±1.96 | 240 dpi 1.3±2.2 | 270 dpi 1.25±2.5 |
| 0 dpi | NI (2.44±2.83) | † | ns | † | † | † | † | ns | ns | † | † | † | † | † |
| | NBI (2.44±2.83) | † | ns | † | † | † | † | ns | ns | † | † | † | † | † |
| 35 dpi | NI (2.47±2.86) | † | ns | † | † | † | † | ns | ns | † | † | † | † | † |
| | NBI (2.46±2.85) | † | ns | † | † | † | † | ns | ns | † | † | † | † | † |
| 90 dpi | NI (2.41±2.8) | † | ns | † | † | † | † | ns | ns | † | † | † | † | † |
| | NBI (2.42±2.81) | † | ns | † | † | † | † | ns | ns | † | † | † | † | † |
| 270 dpi | NI (2.5±2.87) | † | ns | † | † | † | † | ns | ns | † | † | † | † | † |
| | NBI (2.47±2.86) | † | ns | † | † | † | † | ns | ns | † | † | † | † | † |

Differences from controls (NI, non inoculated and NBI, normal brain inoculated at 0, 35, 90 and 270 dpi) were considered statistically significant (*: P<0.05; **: P<0.01; and ***: P<0.001 for student-t test or †, P<0.05; ††, P<0.01; and †††, P<0.001 from Mann-Whitney's-U test).

infectious processes (Aguzzi et al., 2003). These studies, focussing mainly on the CNS, have demonstrated microglial activation, evident both in increased cytokine gene transcription and in the production of IL-1, IL-6, IFN-γ, IL-10 and TNF-α under certain circumstances (Veerhuis et al., 2002; Baker and Manuelidis, 2003; Thackray et al., 2004). However, little is known about the in vivo role of the chemical mediators produced by different immune-system cells at the entry sites for PrPd following oral infection.

The Th1 immune response is characterized by increased production of cytokines such as IFN-γ, induced by TNF-α and IL1-γ (Samuel, 2001; Abbas and Litchman, 2004). The present results showed a significant increase in macrophage TNF-α production, coinciding with maximum intraepithelial macrophage numbers at 15 dpi, suggesting a possible anti-PrPd local inflammatory response mechanism. However, this was not accompanied by an increase in IL-1α production, and few IFN-γ -reactive cells were observed. Afterwards, and despite the highly-significant increase in macrophage numbers detected in lamina propria/submucosa between 60 and 75 dpi, a marked decrease was observed in macrophage synthesis of proinflammatory chemical mediators, mainly TNF-α, which reached minimum values at this stage. This decrease may be related to increased production of IL-10, a cytokine which inhibits the maturation of antigen-presenting cells and the production of proinflammatory cytokines (Abbas and Litchman, 2004). However, no significant increase was noted here in the number of IL-10 positive cells, which would rule out its involvement in a hypothetical inhibition mechanism. Thus, the present results appear to support a possible role of PrPd as an inhibitor of the local immune response, since, as occurs in other infectious processes in which direct action of the agent on immunocompetent cells impairs cell function (Rahman and McFadden, 2006; Winthrop, 2006; Wilson and Crabtree, 2007), the accumulation of PrPd in macrophages would inhibit their capacity to synthesize chemical mediators. Moreover, following PrPd detection in PPs at 60 dpi, some recovery of TNF-α production in lamina propria and submucosa was observed. This finding supports the hypothesis that the local immune response in lamina propria and submucosa may be inhibited during the transport of PrPd to PPs, and that this response may be restored once PrPd is located in PPs. The absence of a significant increase in TNF-α levels in lymphoid follicles further suggests that inhibition of the local immune response may take place at both the transit and accumulation sites, thus favouring the spread of PrPd to other areas.

From the onset of the disease, there was a progressive decrease in the number of IFN-γ-reactive cells in PPs, which reached minimum values between 60-75 dpi, coinciding with the detection of PrPd in these locations. This decrease may be evidence of a functional impairment of T lymphocytes, the main producers of IFN-γ, and thus of the macrophage/lymphocyte costimulation mechanism required to induce an adequate cellular immune response (Abbas and Litchman, 2004; Schoenborn and Wilson, 2007). The possible inhibition of the Th1 response, together with the macrophage chemotaxis reported earlier, could be a key element in the transport of PrPd to the lymphoid tissue. The lack of local inflammatory response in transit and accumulation sites would facilitate the accumulation and subsequent spread of PrPd to the intestinal nerve plexuses, and thence to the brain, a progression confirmed by sequential detection of PrPd in these sites and also reported in other studies of the neural spread of PrPd (Beekes and McBride, 2000; Van Keulen et al., 2000).

The Th2 immune response is characterized by the predominant production of IL-6 and IL-10. On the other hand, the absence of TNF-α and IL-1γ prevents the appropriate stimulation of IL-6-producing cells (Abbas and Litchman, 2004). The results obtained here show that this absence coincided with a lack of IL-10-reactive cells. Thus, the normal development of processes leading to the establishment of a Th2 response would be impeded. Th1 and Th2 immune responses would be affected in the course of the disease and this would allow both the accumulation of PrPd in antigen-presenting cells and the impairment of the microenvironment required for the correct stimulation of T and B lymphocytes. However, further research is required to confirm this hypothesis and to study in depth the exact nature of this mechanism.

*Acknowledgements.* The authors thank José M. Torres (CISA-INIA, Valdeolmos, Madrid, Spain) and Alejandro Núñez (Veterinary Laboratories Agency, Weybridge, Addlestone, Surrey, UK) for kindly supplying the RML infected brains and the polyclonal Rb482 antibody, respectively. We also appreciate the technical assistance of "Servicio Central de Apoyo a la Investigación" (University of Córdoba). This work was financially supported by grants from the Ministry of Education and Science of Spain (EET-2002-05150). P.J. Sánchez-Cordón holds a contract of the "Ramón y Cajal Programme" (Ministry of Education and Science, Spain).

## References

Abbas A.K. and Litchman A.H. (2004). Cellular and molecular immunology. 5th ed. Elsevier Science. Philadelphia.

Aguzzi A., Heppner F.L., Heikenwalder M., Prinz M., Mertz K., Seeger H. and Glatzel M. (2003). Immune system and peripheral nerves in propagation of prions to CNS. Br. Med. Bull. 66, 141-159.

Baker C.A. and Manuelidis L. (2003). Unique inflammatory RNA profiles of microglia in Creutzfeldt-Jakob disease. Proc. Natl. Acad. Sci. USA 100, 675-679.

Beekes M. and McBride P.A. (2000). Early accumulation of pathological PrP in the enteric nervous system and gut-associated lymphoid tissue of hamsters orally infected with scrapie. Neurosci. Lett. 278, 181-184.

Beekes M. and McBride P.A. (2007). The spread of prions through the body in naturally acquired transmissible spongiform encephalopathies. FEBS J. 274, 588-605.

Bons N., Mestre-Frances N., Belli P., Cathala F., Gajdusek D.C. and Brown P. (1999). Natural and experimental oral infection of non-human primates by bovine spongiform encephalopathy agents. Proc. Natl. Acad. Sci. USA 92, 4046-4051.

Brun A., Castilla J., Parra B., Rodríguez F. and Torres J.M. (2003). Involvement of the immunological system in the pathogenesis of transmissible spongiform encephalopathies. Rev. Neurol. 37, 648-653.

Campbell I.L., Eddleston M., Kemper P., Oldstone M.B. and Hobbs M.V. (1994). Activation of cerebral cytokine gene expression and its correlation with the onset of reactive astrocyte and acute-phase response gene expression in scrapie. J. Virol. 68, 2383-2387.

Chesebro B. (2003). Introduction to the transmissible spongiform encephalopathies or prion diseases. Br. Med. Bull. 66, 1-20.

Gauczynski S., Peyrin J.M., Haïk S., Leucht C., Hundt C., Rieger R., Krasemann S., Deslys J.P., Dormont D., Lasmézas C.I. and Weiss S. (2001). The 37-kDa/67-kDa laminin receptor acts as the cell-surface receptor for the cellular prion protein. EMBO J. 20,5863-5875.

Giese A., Brown D.R., Groschup M.H., Feldmann C., Haist I. and Kretzschmar H.A. (1998). Role of microglia in neuronal cell death in prion disease. Brain Pathol. 8,449-457.

Glaysher B.R. and Mabbott N.A. (2007). Role of the GALT in scrapie agent neuroinvasion from the intestine. J. Immunol. 178,3757-3766.

González L., Terry L. and Jeffrey M. (2005). Expression of prion protein in the gut of mice infected orally with the 301V murine strain of the bovine spongiform encephalopathy agent. J. Comp. Pathol. 132, 273-282.

Heppner F.L., Christ A.D., Klein M.A., Prinz M., Fried M., Kraehenbuhl J.P. and Aguzzi A. (2001). Transepithelial prion transport by M cells. Nat. Med. 7, 976-977.

Huang F.P., Farquhar C.F., Mabbott N.A., Bruce M.E. and MacPherson G.G. (2002). Migrating intestinal dendritic cells transport PrPsc from the gut. J. Gen. Virol. 83, 267-271.

Jeffrey M., González L., Espenes A., Press C.M., Martin S., Chaplin M., Davis L., Landsverk T., MacAldowie C., Eaton S. and McGovern G. (2006). Transportation of prion protein accross the intestinal mucosa of scrapie-susceptible and scrapie-resistant sheep. J. Pathol. 209, 4-14.

Kaneider N.C., Kaser A., Dunzendorfer S., Tilg H. and Wiedermann C.J. (2003). Sphingosine kinase-dependent migration of immature dendritic cells in response to neurotoxic prion protein fragment. J. Virol. 77, 5535-5539.

Krüger D., Thomzig A., Lenz G., Kampf K., McBride P. and Beekes M. (2009). Faecal sheeding, alimentary clearance and intestinal spread of prions in hamsters fed with scrapie. Vet. Res. 40, 4.

Maignien T., Shakweh M., Calvo P., Marcé D., Salès N., Fattal E., Deslys J.P., Couvreur P. and Lasmézas C.I. (2005). Role of gut macrophages in mice orally contaminated with scrapie or BSE. Int. J. Pharm. 298, 293-304.

Mishra R.S., Basu S., Gu Y., Luo X., Zou W.Q., Mishra R., Li R., Chen S.G., Gambetti P., Fujioka H. and Singh N. (2004). Protease-resistant human prion protein and ferritin are cotransported across Caco-2 epithelial cells: implications for species barrier in prion uptake from the intestine. J. Neurosci. 24, 11280-11290.

Nieznanski K., Podlubnaya Z.A. and Nieznanska H. (2006). Prion protein inhibits microtubule assembly by inducing tubulin oligomerization. Biochem. Biophys. Res. Commun. 349, 391-399.

Pammer J., Cross H.S., Frobert Y., Tschachler E. and Oberhuber G. (2000). The pattern of prion-related protein expression in the gastrointestinal tract. Virchows Arch. 436, 466-472.

Perry V.H., Cunningham C. and Boche D. (2002). Atypical inflammation in the central nervous system in prion disease. Curr. Opin. Neurol. 15, 349-354.

Peyrin J.M., Lasmézas C.I., Haïk S., Tagliavini F., Salmona M., Williams A., Richie D., Deslys J.P. and Dormont D. (1999). Microglial cell responds to amyloidogenic PrP peptide by the production of inflammatory cytokines. Neuroreport 10, 723-729.

Platt A.M.and Mowat A.M. (2008). Mucosal macrophages and the regulation of immune response in the intestine. Immunol. Lett. 119, 22-31.

Prusiner S.B. (1998). Prions. Proc. Natl. Acad. Sci. USA. 95, 13363-13383.

Rahman M.M. and McFadden G. (2006). Modulation of tumor necrosis factor by microbial pathogens. PLoS Pathog. 2, e4.

Raymond C.R., Aucouturier P. and Mabbott N.A. (2007). In vivo depletion of CD11c+ cells impairs scrapie agent neuroinvasion from the intestine. J. Immunol. 179, 7758-7766.

Rescigno M., Lopatin U. and Chieppa M. (2008). Interactions among dendritic cells, macrophages, and epithelial cells in the gut: implications for immune tolerance. Curr. Opin. Immunol. 20, 669-675.

Samuel C.E. (2001). Antiviral action of interferons. Clin. Microbiol. Rev. 14, 778-809.

Schoenborn J.R. and Wilson C.B. (2007). Regulation of interferon-gamma during innate and adaptative immune responses. Adv. Immunol. 96, 41-101.

Thackray A.M., McKenzie A.N., Klein M.A., Lauder A. and Bujdoso R. (2004). Accelerated prion disease in the absence of interleukin-10. J. Virol. 78, 13697-13707.

Van Keulen L.J., Schreuder B.E., Vromans M.E., Langeveld J.P. and Smits M.A. (2000). Pathogenesis of natural scrapie in sheep. Arch. Virol. Suppl. 57-71.

Veerhuis R., Hoozemans J.J., Janssen I., Boshuizen R.S., Langeveld J.P. and Eikelenboom P. (2002). Adult human microglia secrete cytokines when exposed to neurotoxic prion protein peptide: no intermediary role for prostaglandin E2. Brain Res. 925, 195-203.

Williams A., Lucassen P.J., Ritchie D. and Bruce M. (1997). PrP deposition, microglial activation, and neuronal apoptosis in murine scrapie. Exp. Neurol. 144, 433-438.

Williams A.E., Lawson L.J., Perry V.H. and Fraser H. (1994). Characterization of the microglial response in murine scrapie. Neuropathol. Appl. Neurobiol. 20, 47-55.

Wilson K.T. and Crabtree J.E. (2007). Immunology of Helicobacter pylori: insights into the failure of the immune response and perspectives on vaccine studies. Gastroenterology 133, 288-308.

Winthrop K.L. (2006). Risk and prevention of tuberculosis and other serious opportunistic infections associated with the inhibition of tumor necrosis factor. Nat. Clin. Pract. Rheumatol. 2, 602-610.

Accepted February 26, 2010